JOURNAL OF MATERIALS SCIENCE 29 (1994) 3224–3230

Characterization of milled Si_3N_4 powder using X-ray peak broadening and surface area analysis

B. LÖNNBERG
Institute of Chemistry, University of Uppsala, Box 531, S-751 21 Uppsala, Sweden

Si_3N_4 powder has been milled using a planetary ball mill. The specific surface area, crystallite size and lattice distortions were studied as a function of milling time using the Brunauer–Emmett–Teller (BET) technique and X-ray powder diffractometry. The crystallite size decreased rapidly during the first 50 h of milling. Above 170 h no further decrease of the crystallite size occurred. The smallest crystallite size obtained was 0.074 μm. Lattice distortions were small and decreased slightly during the first 50 h of milling. Specific surface area increased linearly with time. Rapid wear of the milling parts occurred during the first 50 h. Increasing the milling time produced only minor wear. The oxygen content increased linearly with milling time. Reaction with the milling fluid produced an increase in carbon content.

1. Introduction

Si_3N_4 is an excellent candidate for high temperature engineering applications due to its unique combination of properties, such as high strength up to high temperatures, low thermal expansion, high wear resistance and good chemical resistance. Si_3N_4 has gained importance during the last few years as stator vanes, rotors, combuster liners, and a variety of liners for hot-gas flow through turbines and engines [1–3].

The properties of dense Si_3N_4 depend to a large extent on the preparation and processing of the starting powder. Most of the powder prepared commercially is made by the reaction of silicon metal powder with nitrogen at temperatures in the range 1250–1400 °C. The powder is loosely bonded and must be crushed and sized before use. The main drawback is the large amount of pores (20–25%) retained within the powder. High purity Si_3N_4 with small grain sizes can be obtained by carbothermal reduction of SiO_2 in an appropriate nitrogen environment and by the reaction of $SiCl_4$ or silanes with ammonia. Si_3N_4 can also be prepared by chemical vapour deposition (CVD) of products between silicon halides and ammonium [1–3]. Impurities, mainly Fe, Al, Ca, O, C, Cl, are difficult to avoid during preparation. The type and amount of impurities obtained depend on the preparation method used.

The difficulty in sintering pure Si_3N_4 originates from the fact that Si_3N_4 contains strong covalent Si–N bonds, which hinder diffusibility [1, 4]. To achieve sufficient densification, the use of additives, mainly MgO and Y_2O_3, is necessary. The additives produce a liquid phase at high temperatures and thereby promote densification by a liquid phase sintering process.

The sintering reaction can be promoted further by increasing the energy content of the starting powder. The stored energy of the powder normally consists of surface energy and strain energy. The reduction of the powder size is, therefore, an important step in Si_3N_4 preparation and processing.

Several factors, such as the type of mill used, type of milling fluid, amount of powder, etc., influence comminution of the powder. The most commonly used mills are ball mills, vibratory ball mills and attrition mills [4–7]. The attrition and vibratory mills produce more rapid comminution, but have a fairly large impurity pick-up from mill and media wear [6]. Wet grinding is superior to dry grinding since it gives better comminution and produces less agglomeration of the powder. However, dry grinding induces less contamination of the powder [8, 9]. Alcohol is superior to water as a milling fluid, since water produces hydrolysis of the Si_3N_4.

The powder size is normally determined from surface area measurements. These are usually performed using the Brunauer–Emmett–Teller (BET) technique. The BET apparatus determines the total specific surface area of the powder by calculating the amount of nitrogen adsorbed on the surface [10]. The crystallite size can be determined by X-ray diffraction and shows the fragmentation of the powder, i.e. the domains determined by dislocations, grain boundaries and possibly by stacking faults. Crystallite size can, therefore, be used to estimate the dislocation density [11–15]. This X-ray diffraction technique is one of the few methods available for the separation of crystallite size and lattice distortion. Information about crystallite size and lattice distortion is obtained from the broadening of X-ray peaks [16]. The basis for the separation of the two contributions is the dependence of the different angles of the two broadening effects. Several, but at least two, diffraction peaks must therefore be measured. The X-ray method has optimum sensitivity with mean crystallite sizes less than about 0.3 μm [17–20].

0022–2461

To obtain a pure ceramic powder, usually the use of the same type of material in jar and media, as the powder to be milled, is needed. However, in studying milling and wear characteristics in general, other grinding equipment may be used.

The present investigation deals with the milling of Si_3N_4 in a planetary ball mill. Due to counter-movement of the rotating grinding jars on a rotating sun disc, extremely high centrifugal forces can be produced, thereby causing rapid reduction of the most difficult materials to the finest particle size. The mill is equipped with a set of jars and balls consisting of stainless steel, chromium steel, sintered alumina, zirconia and hard metal. In the milling of Si_3N_4 it was found that the hard metal impurity produced the least overlap of the X-ray peaks. Hard metal also displays lower abrasivity than other types of grinding media. Hard metal equipment was, therefore, used in the present investigation. The purpose of the present investigation was to characterize milled Si_3N_4 as regards specific surface area, crystallite size and lattice distortion. The wear characteristics were also studied.

2. Experimental procedure

2.1. Powder characterization and milling procedure

The as-received powder was a commercially available Si_3N_4 powder. The samples were analysed chemically for total oxygen, total carbon, cobalt and tungsten. The as-received powder was also analysed for iron, calcium and aluminium. Chemical analyses showed that the unmilled powder contained 0.46 wt % O, 0.20 wt % C, 0.60 wt % W, Fe < 0.01 wt %, Ca < 0.01 wt %, Al < 0.01 wt %. The lattice parameters of the unground sample were $a = 0.775\,28$ (3) nm and $c = 0.561\,99$ (4) nm. The specific surface area was 1.7 $m^2\,g^{-1}$ and the crystallite size, as determined by X-ray diffraction, was 0.23 μm. The amount of β phase was 8.4 ± 0.4 wt %.

The total carbon content was determined using a LECO CS444 instrument, and the total oxygen content using a LECO TC336 instrument. Cobalt, iron, calcium and aluminium were analysed by atomic absorption spectroscopy (AAS). Tungsten was analysed by photometry (yellow thiocyanate complex, $\lambda = 401$ nm).

The lattice parameters and phase compositions were determined by a Guinier–Hägg focusing X-ray powder diffraction camera using Cu$K\alpha_1$ radiation and silicon ($a = 0.543\,106\,5$ nm [21]) as an internal calibration standard. The positions and intensities were measured using an automatic film scanner. The unit cell dimensions were refined by the least squares method using the local program UNITCELL [22].

The β phase content was calculated from Guinier–Hägg X-ray powder diffraction films using the method described by Gazzara and Messier [23] and Petzow and Sersale [24]. The α peaks used were (101), (110), (200), (201), (102), (210) and (301). The β peaks were (110), (200), (101) and (210). Structure factors, Lorentz polarization factors and multiplicity factors needed for the calculations were obtained using the computer program LAZY [25]. The positional parameters used in the program were obtained from References [26] and [27].

Milling was performed using a planetary ball mill (Retsch PM4) equipped with a 50 ml hard metal grinding jar. Three hard metal balls ($\phi = 20$ mm) were used as grinding media. The rotation speeds of the sun disc and the jar were 175 and 310 r.p.m. respectively. The powder (25 g, about half of the jar volume) was ground in 12 ml of ethanol (purity 99.5%) for up to 195 h.

The as-received powder displayed a broad size distribution, containing particles as large as 0.7 mm. The powder was, therefore, milled for 0.5 h to minimize sampling error and thereby obtain a reliable result for the starting powder. This sample is denoted as "unmilled sample" in the following presentation. However, it should be noted that a comparison between the results of this sample and the results of the as-received sample displayed no significant difference. Powder samples for the X-ray analyses were extracted at 6 h intervals during the first 24 h of milling, and thereafter at 24 h intervals. Powder weighing 1.5 g was used for the X-ray analyses. After each X-ray measurement the powder was poured back into the jar to keep the amount of powder fairly constant during milling. More alcohol was added when needed. Specific surface area was investigated using the BET technique, utilizing a Micromeritics FlowSorb II 2300 instrument.

2.2. Measurement of grain size and lattice distortion

Crystallite size and lattice distortion were investigated using a Siemens D-5000 X-ray powder diffractometer with Cu$K\alpha$ radiation operated at a tube voltage of 45 kV and a tube current of 40 mA. A step scan mode was utilized with 0.02 deg 2Θ per step. The time/step was 12 s. The angular 2Θ range investigated was 17–102 deg. The Cu$K\alpha_2$ contribution was eliminated using the Siemens integrated software package (DIFFRAC-AT). Seven peaks were investigated (Table I).

Split Pearson VII functions were used to describe the peaks. Splitting the Pearson function (Equation 1) into two halves, with a common Bragg angle, 2Θ, and peak intensity, Y_0, allows for the modelling of asymmetric line shapes produced by the diffractometer. Separation of overlapping peaks was obtained using the Siemens integrated software package

TABLE I Diffraction peaks used

hkl	2Θ (deg)	*d* (nm)	Intensity
101	20.59	0.430 99	1000
211	38.91	0.231 30	413
301	43.49	0.207 93	389
222	57.73	0.159 56	98
321	62.46	0.148 56	300
323	80.69	0.118 99	105
205	92.57	0.106 47	30

(DIFFRAC-AT).

$$Y = Y_0\{1 + c_p[(x - x_0)/h]^2\}^{-m} \quad (1)$$

where Y_0 is the peak intensity, c_p the constant, x_0 the peak position, h the peak halfwidth and m is a variable constant.

The full width at half maximum (FWHM) was measured. The data were corrected for instrumental broadening using a certified sample of LaB_6 as a standard reference material (SRM 660). The sample was purchased from The National Institute of Standards and Technology (NIST), Gaithersburg, USA (1989).

3. Results and discussion

Crystallite size and lattice distortion were determined using the method described by Williamson and Hall [11]. The basis for the separation of crystallite size and lattice distortion is the different angular dependence of the two broadening effects. Peak broadening due to small grain size, D, can be described by Scherrer's equation (see Equation 2) [28]

$$B_D = K\lambda/(D\cos\Theta) \quad (2)$$

where B_D is the peak halfwidth, K the shape factor, λ the X-ray wave length and Θ the Bragg angle.

Lattice distortions, $\Delta d/d$, can be obtained by differentiating the Bragg equation:

$$B_d = 4\Delta d/d \tan\Theta \quad (3)$$

where B_d is the peak halfwidth due to lattice distortion.

The components, B_D and B_d, can be combined in various ways to give the total broadening, B_{tot}. The values obtained from peak broadening analysis are largely relative values and depend upon the analytical method used. However, using the same method in all the calculations, the variation of grain size and lattice distortion can be measured. In the present investigation, the Cauchy expression was used, i.e. total broadening is the sum of B_D and B_d.

Addition of the two expressions for peak broadening gives

$$B_{tot} = B_D + B_d = K\lambda/(D\cos\Theta) + 4\Delta d/d\tan\Theta \quad (4)$$

Rearranging the equation gives

$$B_{tot}\cos\Theta = K\lambda/D + 4\Delta d/d\sin\Theta \quad (5)$$

Thus, by plotting $B_{tot}\cos\Theta$ versus $\sin\Theta$ it is possible to obtain D from the intercept and $\Delta d/d$ from the slope.

No systematic deviation of the broadening of the peaks, corresponding to an asymmetric decrease in grain size, could be seen. The grains were, therefore, assumed to be spherical, giving the shape factor $K = 1.0747$ [28].

Before using the halfwidths to calculate the grain size and lattice distortion, the peaks must be corrected for instrumental broadening, b. It has been found that lattice distortions are best approximated by a Gauss distribution, $\beta = B^2 - b^2$, while crystallite size is best approximated by a Cauchy distribution, $\beta = B - b$. When peak broadening is caused by reduction in crystallite size and lattice distortion simultaneously, an empirical formula has proved to give a very good approximation for separation of the instrumental broadening, $\beta = B - b^2/B$ [17].

In the present investigation, it was found that the lattice distortions were very small. Thus, peak broadening is mainly caused by decrease of the crystallite size. The Cauchy approximation was, therefore, used as a correction method.

In total, 12 milling times were studied. Five representative slopes are shown in Fig. 1. Plotting all the corresponding slopes would give a too clustered plot of the measured points. A linear relationship was determined from least squares regression analysis of the data. It is seen that the measured data display small deviations from the slopes, giving a correlation factor, $r^2 > 0.92$. At large milling times, the intensity of the (2 0 5) peak became very low and was, therefore, omitted. An increasing value of the intercept on the $\beta\cos\Theta$ axis indicates that the grain size decreases with increasing milling time. Fig. 2 shows the crystallite size versus milling time. It is seen that a rapid decrease in crystallite size occurs during the first 30 h of milling. The rate of comminution decreases rapidly, and above 170 h the crystallite size reaches a constant value of 0.074 μm. The low rate of comminution at large milling times probably originates from the fact that a reduction of the grain size decreases the probability of Si_3N_4 particles being involved in a collision with the grinding media [6].

As mentioned earlier, the grain size obtained by X-ray diffraction mainly represents the crystallite size determined by dislocation and grain boundaries [12]. Assuming that the crystallite size, D, is the average distance between two dislocation lines, Fig. 2 can be used to calculate the variation in dislocation density.

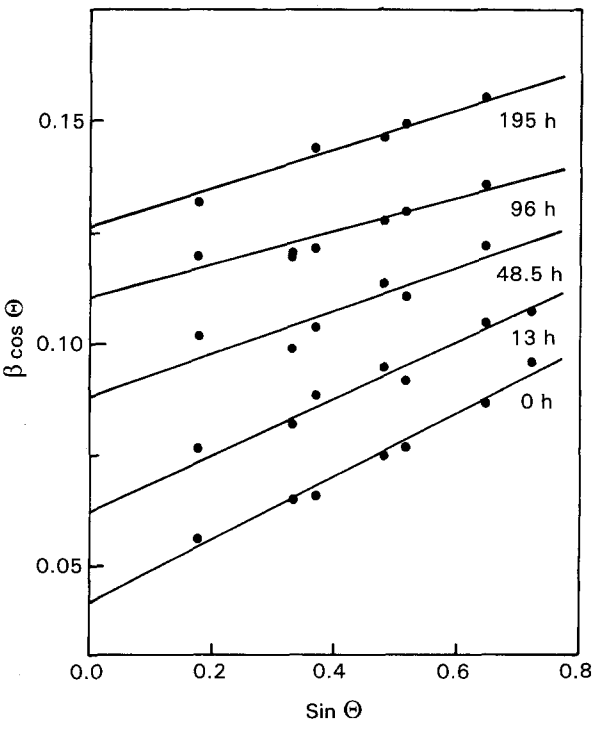

Figure 1 $\beta\cos\Theta$ versus $\sin\Theta$ at various milling times.

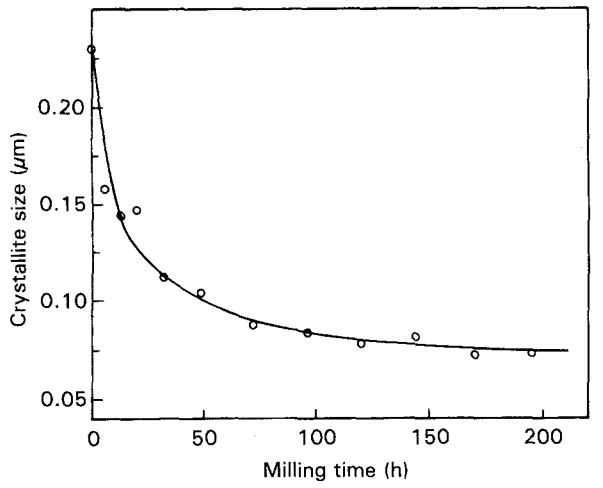

Figure 2 Crystallite size versus milling time.

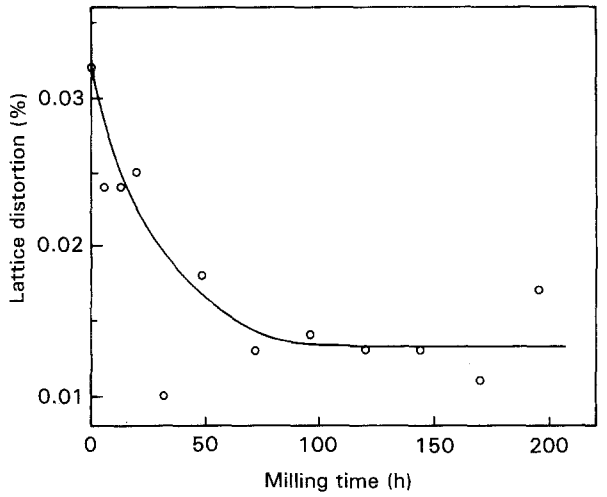

Figure 3 Lattice distortions versus milling time.

The dislocation density can be estimated by the formula, $\rho_D = 3n/D^2$, where n is the number of dislocations per crystallite surface [12]. To utilize the equation, n has to be determined or assumed. In annealed samples, or in very heavily deformed materials in which the dislocations are very nearly random, few dislocations per block surface exist corresponding to a value of n near 1. Deformations in between the two extremes produce larger tilts between the crystallites, corresponding to a larger number of dislocations per crystallite face. In the present investigation, one dislocation per surface has been assumed for simplicity. The calculated values thus represent the minimum dislocation densities present in the powder. The calculations give a dislocation density, $\rho_D = 5.7 \times 10^9$ cm^{-2} for the unmilled powder and a dislocation density, $\rho_D = 5.4 \times 10^{10}$ cm^{-2} for the powder milled for 195 h. These values indicate a high degree of deformation.

Fig. 3 shows the lattice distortion, $\Delta d/d$, versus milling time. It is seen that the distortions decrease unexpectedly during the first 70 h of milling. Usually, increased milling will *introduce* distortions in the powder. It is seen that the unmilled powder contains a lattice distortion of 0.032%. During the first 70 h the distortions decrease to 0.013%. Further milling produced no significant change of the lattice distortions. The high dislocation density, together with the low value of stored elastic strain, suggests that the dislocations are arranged in configurations that reduce their strain energy. Such a configuration could be a polygonized arrangement of the dislocations, i.e. the dislocations move from their slip planes to form bend planes causing their long range stress fields to cancel [11–13]. A contributing factor to the low strain due to partial amorphization of the powder cannot be excluded [4]. However, the diffraction peaks remained sharp at the largest milling time investigated.

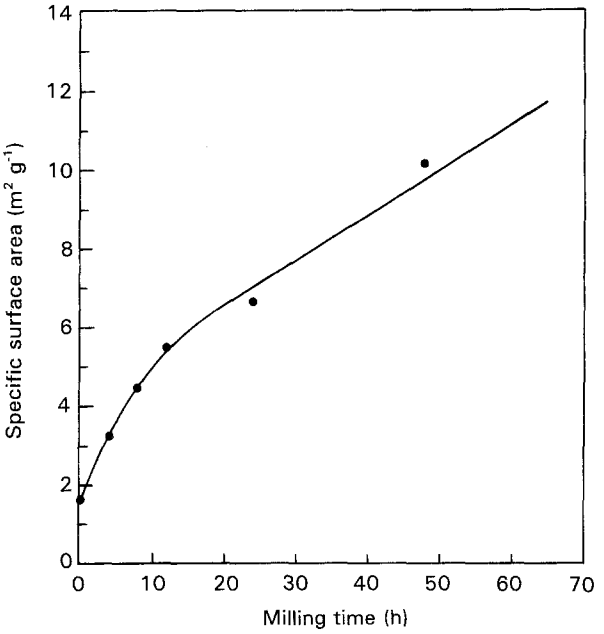

Figure 4 Specific surface area versus milling time.

The strain energy can be calculated using the method described by Faulkner [29]. Assuming a Young's modulus of 304 GPa and a Poisson's ratio of 0.24 [1], the calculation gives a stored strain energy of 0.028 J g^{-1} in the unmilled sample and 0.004 J g^{-1} in samples milled for more than 70 h.

Fig. 4 shows a plot of the specific surface area for up to 50 h milling. It is seen that rapid increase of the specific surface area occurs during the first 10 h of milling. Above 10 h, the rate decreases and becomes linear. The linear increase suggests a low agglomeration rate. This is expected since covalency of the Si–N bond results in low diffusibility of the atoms, corresponding to large activation energy for regrowth [4].

Impurities such as oxygen and carbon will affect the specific surface energy of Si_3N_4. An exact value for the specific surface energy is, therefore, difficult to establish. However, a reasonable order of magnitude is 1 J m^{-2}. Using this value, an increase in the surface energy from about 2 J g^{-1} to about 15 J g^{-1} in milling for 50 h is obtained. Obviously, the surface energy is much larger than the strain energy, and gives the main contribution to the total energy.

Several investigations on the milling of Si_3N_4 have been performed [4–9]. Mostly, attrition and vibration mills have been used. Fig. 5 shows a comparison between the present results and the results of milling experiments on Si_3N_4 reported in Reference [6]. It is

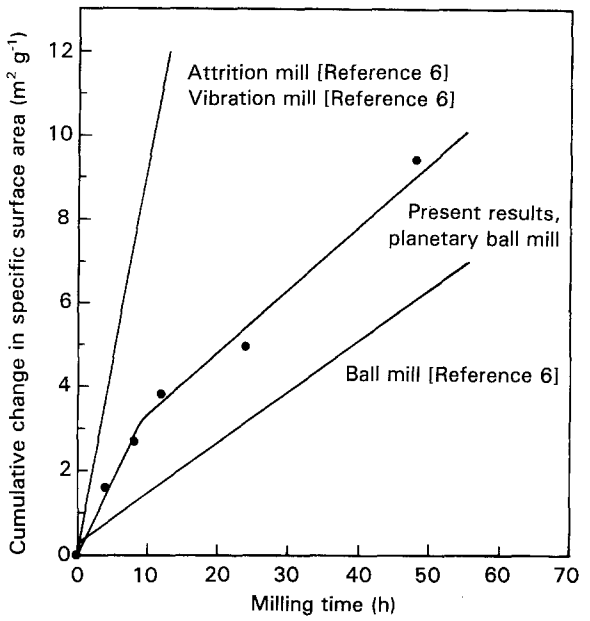

Figure 5 Cumulative change in specific surface area versus milling time. Comparison with literature data.

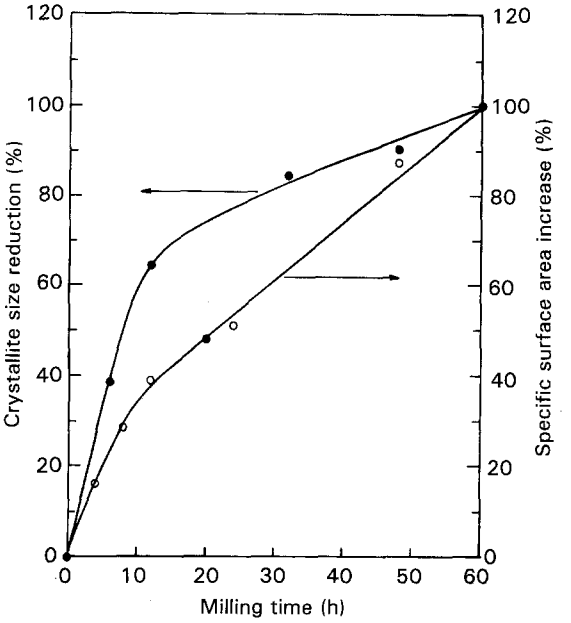

Figure 6 Relative crystallite size and relative specific surface area versus milling time.

seen that ball mills are less efficient than attrition and vibration mills. The planetary ball mill is more effective than the conventional ball mill during the first 10 h of milling. Above 10 h the two ball mills produce similar comminution rates. According to Reference [7] the amount of powder should be fairly small (5–15 vol %) for high grinding efficiency. In the present investigation, the amount of powder (50 vol %) was much larger than the amount used in Reference [6]. It is possible that the fluid to powder ratio can be optimized further. Investigations to optimize the ratio would be of interest. To be able to compare the rate of change of crystallite size and specific surface, the relative *decrease* of crystallite size and the relative *increase* of surface area, up to 60 h of milling, were calculated (Fig. 6). It is seen that the crystallite size changes more rapidly during the first 10–15 h of milling than does the specific surface area. The specific area displays a less, but fairly linear increase. Thus, the crystallite size and specific area do not decrease and increase, respectively, at the same relative rate. The energy produced by milling results in a rapid increase in the number of domains. Breaking the particles requires more energy, resulting in a lower increase in surface area. The results of the chemical analyses are shown in Figs 7–9. It is seen that substantial wear of the grinding jar and media occurs (Fig. 7). A rapid increase of the impurities occurs during the first part of the milling. A maximum of 16.25 wt % hard metal impurity was found in the sample. The wear decreases with grinding time and becomes very small above 150 h milling time. This can be ascribed to the reduction of particle size, leading to less interaction between Si_3N_4 particles and the grinding media.

Subtraction of the carbon needed for stoichiometric WC reveals that excess carbon has been introduced into the powder (see Fig. 8). Above 20 h milling time the amount of excess carbon increases linearly with milling time. The amount of free carbon at 195 h milling is 1.35 wt %. The carbon comes most probably

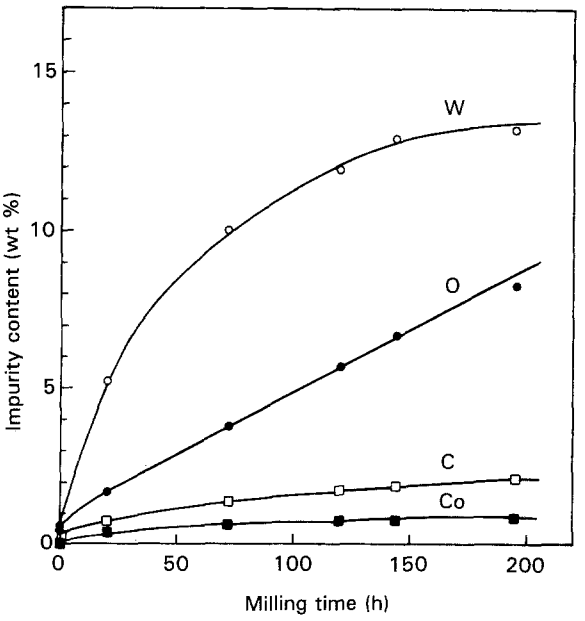

Figure 7 Impurity content versus milling time.

from reaction with the milling fluid [5]. It was also noted that overpressure existed when the milling jar was opened. Small amounts of ammonia were produced during milling, which obviously originated from hydrolysis of Si_3N_4 due to the small quantities of water present in the ethanol.

It is seen in Fig. 7 that the oxygen content increases linearly with milling time, a fact which to a large extent can be ascribed to the increasing surface area [5]. A certain amount of oxygen promotes densification by increasing the amount of liquid phase formed during sintering. However, low oxygen contents are required to obtain good mechanical properties [2]. Fig. 9 shows oxygen content as a function of surface area. It is seen in that the oxygen content increases proportionally with specific area. The oxygen pick-up,

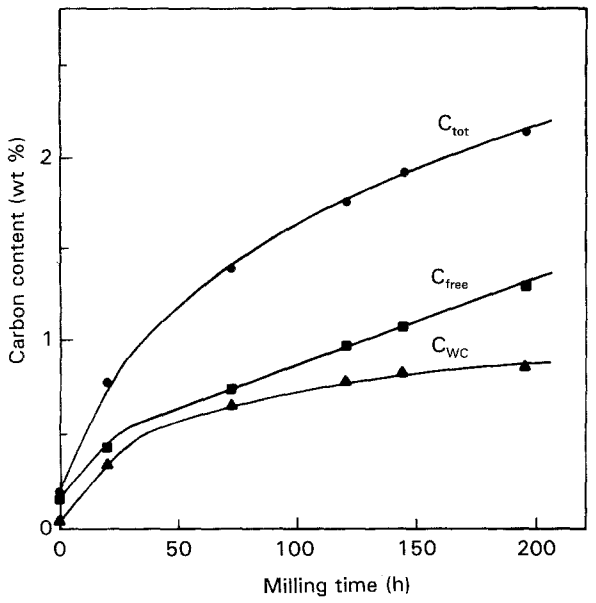

Figure 8 Carbon content versus milling time.

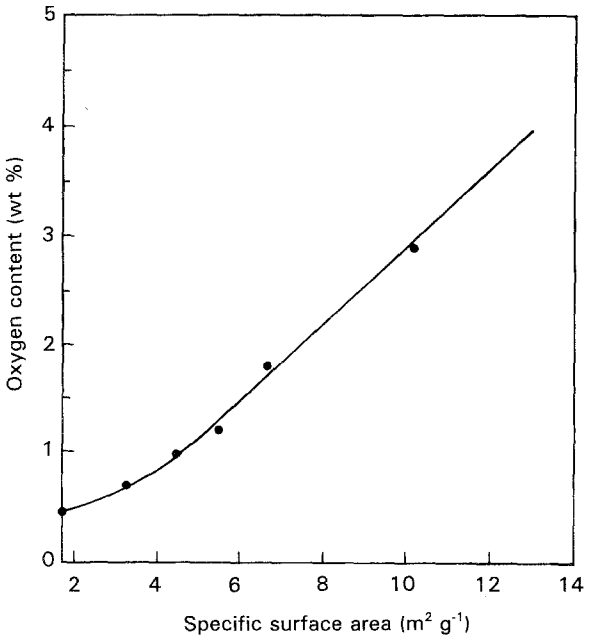

Figure 9 Oxygen content versus specific surface area.

(0.30 wt % m^{-2} g^{-1}), is unexpectedly large. It is possible that the high energy produced by the planetary ball mill increases the slurry temperature and causes increased oxidation of the powder surface [6]. It is also possible that some oxygen has been retained within the structure. However, the lattice parameters of the α-Si_3N_4 remained the same in all the milled samples. No signs of orthorhombic Si_2N_2O could be seen on the X-ray films.

4. Conclusions

The Si_3N_4 powder has been milled up to 195 h using a planetary ball mill equipped with a hard metal grinding jar and media. The milling fluid was ethanol.

The crystallite size decreased from 0.23 μm in the unmilled sample, to 0.074 μm in the 195 h milled sample. Lattice distortion decreased from 0.032 to 0.013% during the first 70 h of milling. A polygonial arrangement of the dislocations is assumed. The dislocation density of the maximum milled sample was $\rho = 5.4 \times 10^{10}$ cm^{-2}, corresponding to a severely deformed powder. The increase in total energy consisted mainly of surface energy; the specific surface increased linearly with time. Wear of the milling jar and media was substantial, leading to 16.25 wt % hard metal impurity in the sample milled for 195 h. The increase in oxygen content was linear with milling time. This increase is to a large extent due to increasing surface area. Free carbon was introduced due to reaction with the milling fluid.

Acknowledgements

The author wishes to thank Docent Torsten Lundström for valuable discussions. Thanks to Professor Bertil Aronsson, AB Sandvik Hard Materials for supplying the Si_3N_4 powder. Mrs Ann-sofi Ullström is gratefully acknowledged for her assistance in BET measurement. The author is indebted to Dr Jan Qvick and SECO Tools AB for carrying out the chemical analyses. Partial financial support from the Swedish Natural Science Research Council is gratefully acknowledged.

References

1. D. W. RICHERSON, "Modern Ceramic Engineering", (Marcel Dekker, New York, 1982) p.126.
2. G. WÖTTING and G. ZIEGLER, *Interceram.* **35** (1986) 32.
3. I. J. MCCOLM, "Ceramic Science for Materials Technologists", (Chapman and Hall, New York, 1983) p. 107.
4. Y. KANNO, *Powder Met.* **44** (1985) 93.
5. T. P. HERBELL, T. K. GLASGOW and N. W. ORTH, *Ceramic Bulletin* **63** (1984) 1176.
6. T. P. HERBELL, M. R. FREEDMAN and J. D. KISER, *Ceram. Eng. Sci. Proc.* **7** (1986) 817.
7. M. R. FREEDMAN, J. D. KISER and T. P. HERBELL, *ibid.* **6** (1985) 1124.
8. L. T. GANKEVICH, S. G. TITOV, S. L. BOCHKOV, K. K. UZBEKOVA, E. M. CHEREDNIK and A. F. KUTEINIKOV, *Poroshk. Metall.* **9** (1987) 1.
9. K. SUZUKI and Y. KUWAHARA, *Kona* **2** (1984) 2.
10. B. C. LIPPENS and M. E. A. HERMANS, *Powder Met.* **7** (1961) 66.
11. G. K. WILLIAMSON and W. H. HALL, *Acta Met.* **1** (1953) 22.
12. G. K. WILLIAMSON and R. E. SMALLMAN, *Phil. Mag.* **1** (1956) 34.
13. M. J. KLEIN and P. S. RUDMAN, *ibid.* **14** (1966) 1199.
14. K. R. EVANS and W. F. FLANAGAN, *ibid.* **14** (1966) 1131.
15. R. W. HECKEL and J. L. YOUNGBLOOD, *J. Amer. Ceram. Soc.* **51** (1967) 398.
16. N. F. M. HENRY, H. LIPSON and W. A. WOOSTER, "The Interpretation of X-ray Diffraction Photographs", (Macmillan, London, 1960) p. 212.
17. G. ZIEGLER, *Powder Met. Int.* **10** (1978) 70.
18. *Idem., Keram. Z.* **33** (1981) 287.
19. *Idem., ibid.* **33** (1981) 602.
20. T. EKSTRÖM, C. CHATFIELD, W. WRUSS and M. MALY-SCHREIBER, *J. Mater. Sci.* **20** (1985) 1266.
21. R. D. DESLATTES and A. HENINS, *Phys. Rev. Lett.* **31** (1972) 972.
22. B. NOLÄNG, unpublished, Institute of Chemistry, University of Uppsala, (1990).
23. C. P. GAZZARA and D. R. MESSIER, *Ceramic Bulletin* **56** (1977) 777.

24. G. PETZOW and R. SERSALE, *Pure & Appl. Chem.* **59** (1987) 1673.
25. K. YVON, W. JEITSCHKO and E. PARTHE, *J. Appl. Crystallogr.* **10** (1977) 73.
26. R. MARCHAND, Y. LAURENT and J. LANG, *Acta Cryst.* **B25** (1969) 2157.
27. O. BORGEN and H. M. SEIP, *Acta Chem. Scand.* **15** (1961) 1789.
28. H. P. KLUG and L. E. ALEXANDER, "X-ray Diffraction Procedures for Polycrystalline and Amorphous Materials", (Wiley, New York, 1974) p. 659.
29. E. A. FAULKNER, *Phil. Mag.* **5** (1960) 519.

Received 2 July
and accepted 16 December 1993